TEKA. COMMISSION OF MOTORIZATION AND ENERGETICS IN AGRICULTURE – 2013, Vol. 13, No. 1, 65–70

Employing empirical mode decomposition to determine solar radiation intensity curve

Jacek Kapica, Marek Ścibisz

University of Life Sciences in Lublin, Doświadczalna 50A, 20-280 Lublin
email: jacek.kapica@up.lublin.pl, marek.scibisz@up.lublin.pl

Received January 25.2013; accepted March 14.2013

Summary. The paper presents an application of the empirical mode decomposition to filtering of the fast changing components of the solar radiation curve. Results of the measurement of the solar irradiation for a few typical days are presented. The measurements were taken with a frequency of one sample per second, which is a high value as for solar radiation. Then the data were resampled with lower sampling frequencies, directly and after eliminating fast changing components with the use of empirical mode decomposition. For each case a daily solar energy was calculated.
Key words: empirical mode decomposition, signal filtration, solar radiation.

INTRODUCTION

Since the energy crisis in 1970's a constant growth of photovoltaic power production has been observed [6, 12, 16]. One of the areas of solar energy application is agriculture [13, 17]. This kind of energy is sometimes considered as "agro-energy" [14].

The solar radiation, depending on the weather conditions on a particular day, may have various levels of variability. On a cloudless day or when the sky is covered with evenly distributed cloud layer, the insolation changes slowly according to the earth rotation. But on a windy day when the sky is covered with small clouds (for example cumulus clouds), the radiation changes very quickly.

Due to the shape of the current – voltage curve of the photovoltaic (PV) panels, the efficiency of the set PV generator – electrical load depends on how the load matches the source. In systems with battery, instantaneous values of the solar insolation are not that important – presence of the battery stabilizes the working point of the generator. A different situation, due to aforementioned problem of matching between generator and load, occurs in case of a PV island system without battery. It is of special importance in case of applications in agriculture, where this kind of PV system may be employed.

Therefore, when analyzing the operation of systems powered by photovoltaic generators, it often happens that in addition to the sum of energy in a given day the calculations are performed using the data from measurements of the instantaneous values of radiation intensity (as in [15]). The highest accuracy is achieved by using high sampling frequencies, but such an approach generates huge amounts of data which in case of long lasting measurements can be inconvenient because of the storage space required and CPU usage when this data is used in computer simulations. The solution is to properly choose the sampling frequency, however the sampling points are chosen randomly and it may happen that that the sample will be taken in a moment which is not representative for a given period, for example in a temporary, short moment of cloudiness.

An alternative approach is to acquire the data with high frequency, process it in order to eliminate (average) the high volatility and then to resample it with lower frequency for data archiving.

The paper presents application of Empirical Mode Decomposition (EMD) to filter fast changing components of solar radiation curve.

EMPIRICAL MODE DECOMPOSITION

Empirical mode decomposition (EMD) is a novel method which can be applied to any complicated data set in order to decompose it into a finite number of intrinsic mode functions. It is applicable to non-linear and non-stationary processes [1, 4, 5].

According to Huang [8] the decomposition is made on an assumption that any data consists of different simple intrinsic modes of oscillations. Each of the oscillatory modes is represented by an intrinsic mode function (IMF) with the following definition [7]:

1. in the whole data set, the number of extrema and the number of zero crossings must either be equal or differ at most by one;
   and
2. at any point, the mean value of the envelope defined by the local maxima and the envelope defined by the local minima is zero.

An integral part of the EMD procedure is the sifting process. It can be described by the following steps, assuming that $x(t)$ is the source data:

1. Find all the local extrema (minima and maxima) of $x(t)$,
2. Interpolate the extrema with a cubic spline: the maxima will create the upper envelope *eup_n*(t), the minima will create the lower envelope *elo_n*(t),
3. calculate the mean value line which lies between the upper and lower envelope according to the following equation:

$$m_n = \frac{e_{up\_n}(t) + e_{lo\_n}(t)}{2}, \tag{1}$$

4. calculate the residue *hn*:

$$h_n = x(t) - m_n, \tag{2}$$

5. the steps 1 to 4 are repeated treating *hn* as the input data until a stoppage criteria is met.

There are two approaches to the stoppage criteria. One is to calculate normalized squared difference between two successive sifting iterations n and n-1 [8]:

$$SD_n = \frac{\sum_{t=0}^{T} |h_{n-1}(t) - h_n(t)|^2}{\sum_{t=0}^{T} h_{n-1}^2}, \tag{3}$$

and continue the iterations until the *SDn* is small enough. This criterium, however, does not guarantee that the function will have the same number of zero-crossings and extrema, even if the value of *SDn* is lower than a given threshold value.

Another stoppage criterium proposed in [9] is based on the fact whether the signal obtained in the last iteration has the same number of zero-crossings and extrema. With this criteria, the sifting process will stop only after S consecutive times when the number of extrema and zero-crossings differ at most by one. The value of S proposed by Huang et al. is between 4 and 8 for optimal sifting.

If the stopping criteria is met the *hn* will be the first IMF which represents the fastest oscillating component. Subtracting $x(t)$ and *IMF1* gives the residue *r1*:

$$r_1 = x(t) - IMF_1, \tag{4}$$

r1 contains longer oscillations and is treated as input data to the sifting process. In this manner the following IMFs are computed until *IMFn* or *rn* becomes smaller than a predefined value or when *rn* becomes a monotonic function.

Considering equation (4) and iterative nature of the procedure we may write that:

$$x(t) = \sum_{j=1}^{n} IMF_n + r_n. \tag{5}$$

The equation (5) reflects the decomposition process of the given signal $x(t)$ into a series of n IMFs and the residue. Each higher IMF represents longer oscillating component of $x(t)$. The procedure is illustrated on figure 1.

As the intrinsic mode functions of various orders represent different levels of oscillations, eliminating the components with shorter oscillations can be used to filter-out the fast changing components of a given signal.

One big advantage of decomposing the signal using the empirical mode decomposition is that there is no need to decide apriori which function will be used to represent the signal. In contrast, in traditional Fourier transform a sinusoidal function is assumed and in wavelet transform the mother function needs to be chosen prior to the analysis.

Several authors have addressed the usage of the EMD in solar radiation analysis [11, 18, 19, 20]. None of them however uses the EMD to filter solar radiation data. Some attempts are made to employ this procedure to filter other kinds of signals. Fleureau and others [5] use a modified version of EMD to filter ElectroEncephaloGraphic(EEG) sleep recording.

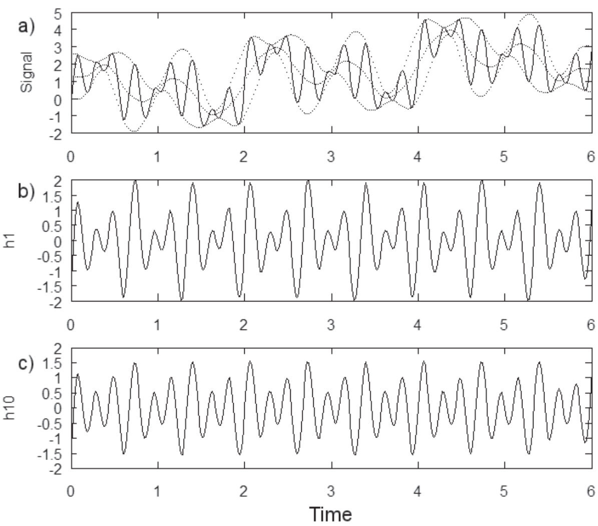

Fig. 1. Example of a sifting process for a simulated signal. a) original signal (solid line), upper and lower envelopes with mean line (dotted lines), b) result of the first iteration of the sifting, c) result of the 10th iteration of the sifting

DATA, METHODS AND TOOLS

The short-circuit current of a photovoltaic cell is directly proportional to insolation [10]. This fact has been used to measure the solar radiation intensity on a PV module plane. The diagram of the measurement circuit is presented on Fig. 2. The sampling frequency was 1 sample per second, which is a high value for solar radiation measures. The measurement was made with help of an application created in a LabView programming environment which is suitable for measurements both in real and simulated circuits [2, 3].

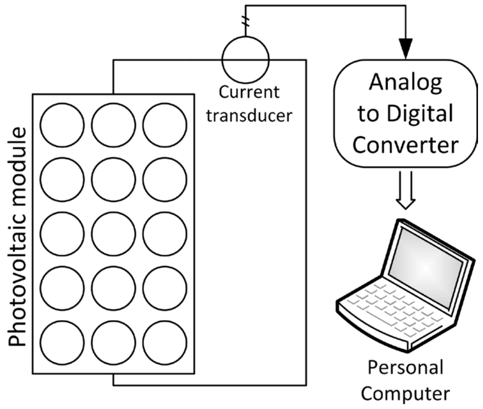

Fig. 2. Diagram of the circuit for solar insolation measurement

The next step was to obtain two types of signals: 1) a signal created by resampling of the original signal with lower frequency, 2) a signal created after filtering the fast-changing components of the originally measured signal and resampling it with the same frequency as the first signal. These steps were performed by a script executed in the GNU Octave programming environment [4]. The script was also calculating the daily amount of solar energy by using a signal acquired with frequency of one sample per second and the two types of signals described previously. Also the absolute and relative errors of daily energy estimation were calculated with an assumption that the original signal is error-free.

The filtering consists of the following steps:

1. Decompose the original signal into set of IMFs,
2. Reconstruct the signal eliminating the IMFs representing faster oscillations.

As a result a new signal is obtained in which the rapid changes of the solar irradiation are removed.

RESULTS

The analyzed data was solar insolation curve registered by the author for selected days of April 2010. Figure 3 presents the instantaneous power of the solar radiation on a PV module plane. On days A and B we can see many rapid changes of the insolation. Day C has significantly less fast components.

The signal was decomposed into 20 intrinsic mode functions plus residue. The filtering was done by reconstructing the signal using higher level IMFs – the IMFs representing faster oscillations were removed. The calculations were done for all the sequences of the IMFs, eliminating the lowest functions gradually (2-20 plus residue, 3-20 plus residue and so on). The results are presented on a 3D chart (Figures 4-6). Additionally, 2D graphs are presented for selected sequences of reconstructed signal (Figures 7-9). For convenience, the residue will be referred as 21st IMF on the charts. On the 3D charts, the presented IMF value is the first IMF included in the signal reconstruction, for example 5 means that the signal is reconstructed from the 5th IMF and higher plus residue.

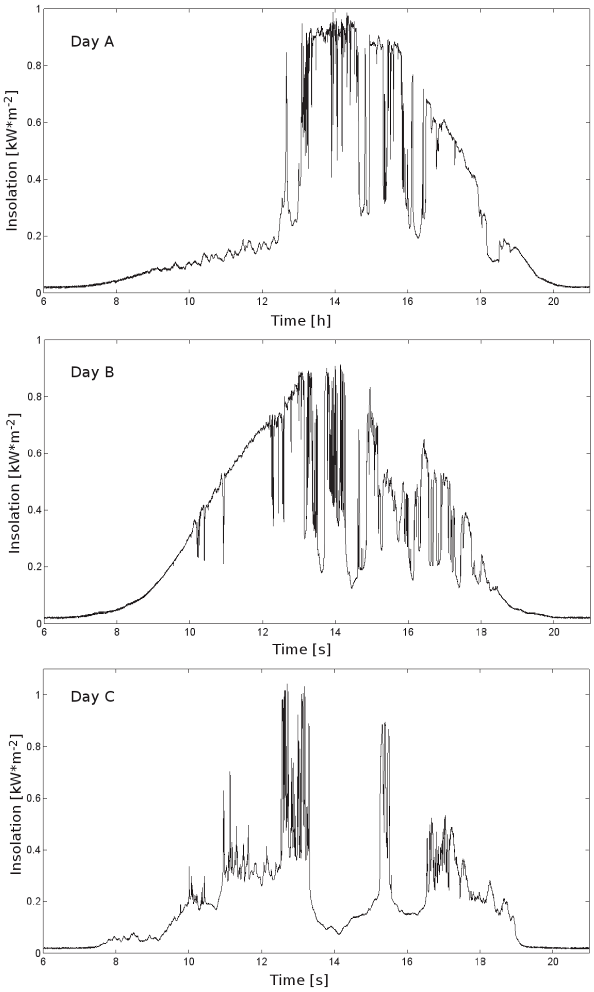

Fig. 3. Solar insolation curve on selected days of April 2010

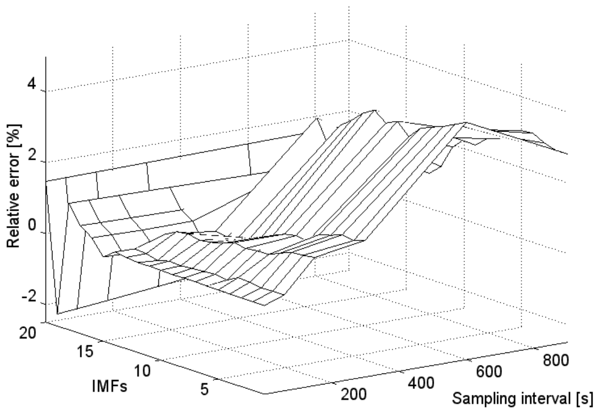

Fig. 4. 3D chart illustrating influence of the IMF components included in the signal reconstruction on the relative error for selected sampling intervals for day A

CONCLUSIONS

The results show that when applying shorter sampling intervals (higher sampling frequency) the error of calculating the daily energy is usually less. There are, however, cases with longer sampling intervals (like 600 and 900 s), in which the relative error is lesser, compared to longer intervals. The

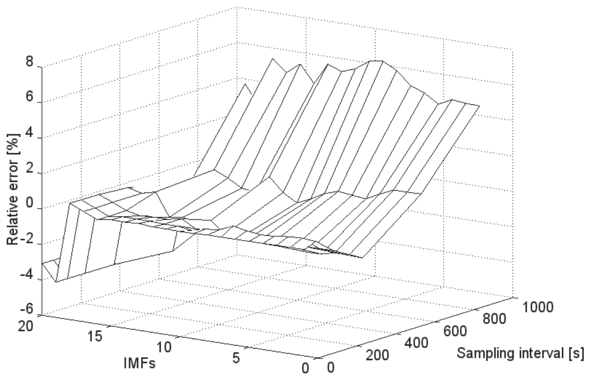

Fig. 5. 3D chart illustrating influence of the IMF components included in the signal reconstruction on the relative error for selected sampling intervals for day B

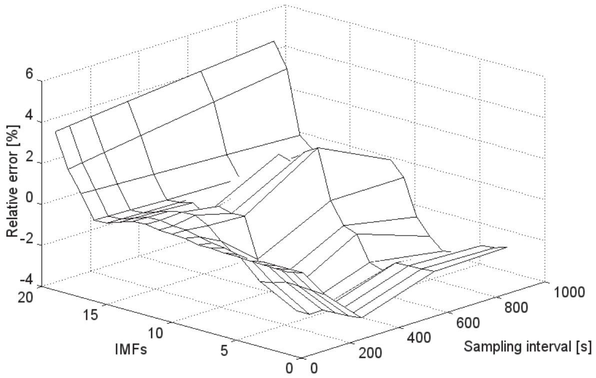

Fig. 6. 3D chart illustrating influence of the IMF components included in the signal reconstruction on the relative error for selected sampling intervals for day C

accuracy of daily energy estimation depends also on the intensity of the irradiation oscillations.

Application of the proposed filtration allowed for an increase of the measurement accuracy. In most cases the error after filtration of the fast-oscillating components is significantly lower than without the filtration, in some cases it is similar. The results show that we should not eliminate too many IMFs – not more than 10 fast oscillating components. Otherwise, the results may become unstable – producing a generally random error.

The relative error values, even without the filtering, are relatively small and not greater than 6 % and if sampling intervals not greater than 3 minutes would be used – not greater than 3,5 %. Nevertheless eliminating faster oscillations with the described procedure decreases the error further.

Applying sampling intervals less than 60 s, even without signal filtering allows for high measurement accuracy. In cases when, due to the amount of the acquired data and calculations performed, it is necessary to use longer sampling intervals it is advisable to perform the measurement with higher frequency, then to remove faster oscillations with the presented method and, before archiving, resample the signal with lower frequency. This will allow for higher accuracy of calculations made using the prepared data.

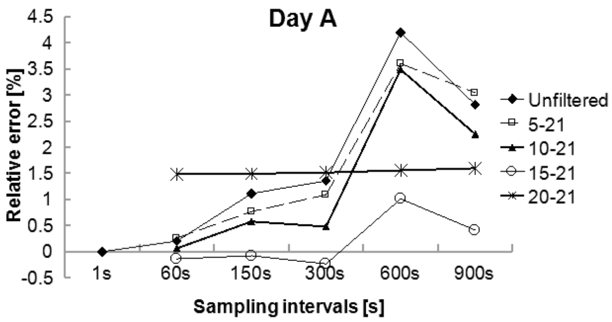

Fig. 7. Illustration of the influence of the IMF components included in the signal reconstruction on the relative error for selected sampling intervals for day A.

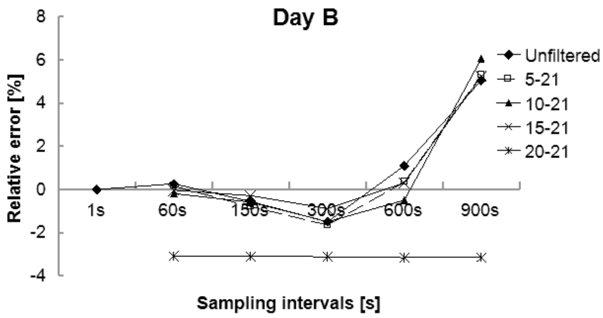

Fig. 8. Illustration of the influence of the IMF components included in the signal reconstruction on the relative error for selected sampling intervals for day B

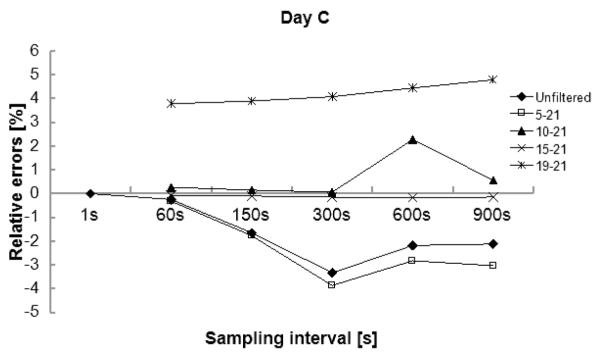

Fig. 9. Illustration of the influence of the IMF components included in the signal reconstruction on the relative error for selected sampling intervals for day C

REFERENCES

1. **Braun S. G., Ewin D. J.; Rao S. S. 2002:** Encyclopedia of Vibration, Volumes 1–3, 647. Elsevier.
2. **Buczaj M., Sumorek A. 2007:** Simulation of motor vehicles instrument panels in LabView environment. Teka Komisji Motoryzacji i Energetyki Rolnictwa VII, 52.
3. **Buczaj M., Sumorek A. 2011:** The use LabView environment for the building of supervision system controlling the climatic and technical parameters in farm rooms. Teka Komisji Motoryzacji i Energetyki Rolnictwa XI, 18.
4. **Eaton J.W., 2000:** GNU Octave Manual, Network Theory Limited, ISBN: 0-9541617-2-6

5. **Fleureau J., Kachenoura A., Albera L., Nunes J.-C., Senhadji L. 2011:** Multivariate empirical mode decomposition and application to multichannel filtering, Signal Processing, Volume 91, Issue 12, 2783–2792
6. **Grubb M., Vigotti R. 1997:** Renewable Energy Strategies for Europe: Electricity systems and primary energy sources. Royal Institute of Internetional Affairs.
7. **Huang, N., Shen, Z., Long, S., Wu, M., & Shih H. 1998:** The empirical mode decomposition and the Hilbert spectrum for nonlinear and non-stationary. Proceedings Mathematical, (454), 903–995.
8. **Huang, Norden E. 2005:** Empirical mode decomposition for analyzing acoustical signals. United States Patent 6862558.
9. **Huang, N. E. 2005:** Introduction to the Hilbert Huang Transform and its related Mathematical problems. (N. E. Huang & S. S. P. Shen, Eds.)Interdisciplinary Mathematics, 5, 1–26.
10. **Kalogirou S. A. 2009:** Solar Energy Engineering – Processes and Systems, 477. Elsevier. ISBN: 978-0-12-374501-9
11. **Lin Z. S., Wang S. G. 2006:** EMD analysis of solar insolation. Meteorology and Atmospheric Physics. Earth and Environmental Science, Volume 93, Numbers 1–2 (2006), 123–128.
12. **Lotsch H.K.V., Goetzberger A., Hoffman V.U. 2005:** Photovoltaic Solar Energy Generation. Springer Series in Optical Sciences Volume 112.
13. **Luque A., Hegedus S. 2003:** Handbook of photovoltaic science and engineering. John Wiley & Sons, 54.
14. **Roszkowski A. 2006:** Agriculture and fuels of the future. Teka Komisji Motoryzacji i Energetyki Rolnictwa VI, 132.
15. **Sarniak M. 2011:** The testing of energy efficiency of a prototype hybrid solar panel. Teka Komisji Motoryzacji i Energetyki Rolnictwa XI, 335–342.
16. **Sinha P.C. 1998:** Energy Crisis. Anmol Publications, 184.
17. **Tiwari G. N., Dubey S. 2010:** Fundamentals of Photovoltaic Modules and their Applications. Royal Society of Chemistry. ISBN: 978-1-84973-020-4, 118.
18. **Xian S., Zhenshan L., Xiaoxia C. Chuangye J. 2008:**Regional features of the temperature trend in China based on Empirical Mode Decomposition, Journal of Geographical Sciences, Volume 18, Number 2 (2008), 166–176.
19. **Yang C X, Wu H F, Hu D T. 2011:** Relationship between air temperature oscillations and solar variability on short and medium time scales. Sci China Earth Sci, Vol. 54, 912–923.
20. **Yong W., Qi-Long M., Chong-Yi E., Jian-Kang H., Yuan-Yuan D. 2010:** Relation between temperature changes of the mid-upper troposphere over Eurasian mid-high latitudes and solar irradiance in the twentieth century. Environmental Earth Sciences, Volume 60, Number 6 (2010), 1257–1266.

ZASTOSOWANIE EMPIRYCZNEJ DEKOMPOZYCJI MODÓW DO WYZNACZANIA KRZYWEJ NATĘŻENIA PROMIENIOWANIA SŁONECZNEGO

Streszczenie: Artykuł przedstawia zastosowanie empirycznej dekompozycji modów do filtrowania szybkozmiennych składowych krzywej natężenia promieniowania słonecznego. Przedstawiono wyniki pomiarów natężenia promieniowania słonecznego dla kilku typowych dni. Pomiary były dokonywane z częstotliwością jednej próbki na sekundę, co jest wartością dużą dla promieniowania słonecznego. Następnie dane zostały ponownie spróbkowane bezpośrednio oraz po wyeliminowaniu szybkozmiennych składowych z wykorzystaniem empirycznej dekompozycji modów. Dla każdego z przypadków została wyznaczona wartość dziennej energii promieniowania słonecznego.

Słowa kluczowe: empiryczna dekompozycja modów, filtracja sygnału, promieniowanie słoneczne.